

RESEARCH ARTICLE

10.1029/2018JA025383

Key Points:

- Collisional heating of interstellar helium atoms results in increase of the LISM temperature derived from helium atom direct detection
- Local interstellar medium appears 175–270 K hotter in observations than it is

Correspondence to:

M. Gruntman,
mikeg@usc.edu

Citation:

Gruntman, M. (2018). Collisional heating of interstellar helium flux at 1 AU. *Journal of Geophysical Research: Space Physics*, 123, 3291–3298. <https://doi.org/10.1029/2018JA025383>

Received 22 FEB 2018

Accepted 23 APR 2018

Accepted article online 30 APR 2018

Published online 11 MAY 2018

Collisional Heating of Interstellar Helium Flux at 1 AU

Mike Gruntman¹ 

¹Department of Astronautical Engineering, Viterbi School of Engineering, University of Southern California, Los Angeles, CA, USA

Abstract Because of relative motion of the local interstellar medium (LISM) with respect to the Sun, the interstellar wind, interstellar neutral helium atoms enter the heliosphere. Instruments on the Ulysses and Interstellar Boundary Explorer spacecraft measured directional dependencies of intensities, or sky maps, of helium atoms and determined the interstellar wind velocity vector and temperature. The article focuses on heretofore unaccounted for heating of inflowing interstellar helium by elastic collisions with the solar wind ions and its effect on the LISM temperature obtained from the Interstellar Boundary Explorer-type measurement. The calculations show that inferred LISM temperatures appear 175–270 K hotter than the actual interstellar gas due to collisions.

Plain Language Summary As derived from measurements of interstellar helium atom fluxes temperature of the local interstellar medium surrounding the Sun appears 175–270 degrees hotter than in reality due to heretofore unaccounted for heating of helium fluxes by elastic collisions with solar wind ions

1. Interstellar Helium in the Solar System

Because of relative motion of the local interstellar medium (LISM) with respect to the Sun, the interstellar wind, interstellar neutral helium atoms enter the heliosphere. The atoms move along hyperbolic trajectories under the gravitational force of the Sun and experience ionization losses.

Direct detection of individual interstellar He atoms has emerged as an important technique to determine the velocity vector and temperature of the LISM. In such experiments, an instrument on a spacecraft measures local direction-dependent atom intensities ($\text{cm}^{-2} \cdot \text{sr}^{-1} \cdot \text{s}^{-1}$), also commonly called directional fluxes. Directional distributions of intensities, or sky maps, depend on the position and velocity of the observer and on the velocity vector, temperature, and number density of helium “at infinity” in the interstellar medium surrounding the Sun.

The experiment GAS (Rosenbauer et al., 1983; Witte et al., 1992) on board the interplanetary Ulysses spacecraft, launched in 1990, directly detected for the first time interstellar helium fluxes (Witte, 2004; Witte et al., 1996). Then, the Earth-orbiting Interstellar Boundary Explorer (IBEX), launched in 2008, measured interstellar helium fluxes at 1 AU (Moebius, Bochsler, et al., 2009). In situ measurements of low-energy neutral atom fluxes could rely on various experimental techniques (Gruntman, 1989, 1993, 1997; Moebius, Kucharek, et al., 2009; Rosenbauer et al., 1983). The He atom instruments on Ulysses (Rosenbauer et al., 1983; Witte et al., 1992, 1999) and IBEX (Fuselier et al., 2009), based on different physical detection processes, obtained interstellar helium properties that are in general but not complete agreement (Bzowski et al., 2012, 2015; Moebius et al., 2012, 2015; Witte, 2004; Wood et al., 2015, 2017).

Two recent IBEX results point to importance of examining heretofore unaccounted for physical processes that may modify observed interstellar helium atom intensities.

First, interpretation of IBEX measurements suggested that the interstellar wind direction had changed by a few degrees during the last 40 years (Frisch et al., 2013) that is on spatial scales smaller than the mean free path of helium atoms in the LISM surrounding the Sun. This consequential conclusion was not universally accepted (e.g., Katushkina et al., 2014; Lallement & Bertaux, 2014; Wood et al., 2015). The further analysis stated that the interstellar wind direction change “remained statistically likely”, but at the same time, a constant flow direction was also “statistically possible” (Frisch et al., 2015). A summary of 6 years of interstellar helium observations by IBEX (Bzowski et al., 2015; McComas et al., 2015) outlined changes in analytical approximations (Lee et al., 2012, 2015; Moebius et al., 2015) used in data analysis, provided a set of inferred parameters of the LISM, and described important interdependence of these parameters due to specifics of IBEX observations.

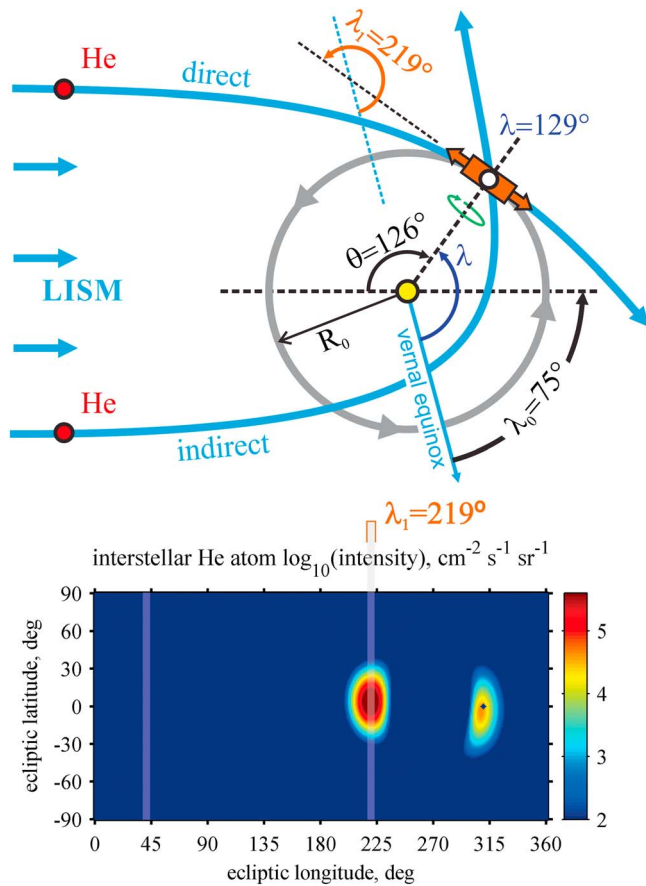


Figure 1. (top) Two trajectories, direct and indirect, of interstellar He atoms with the same velocity in the LISM reach a given point at the earth orbit ($R_0 = 1$ AU). Angle θ is measured from the upwind (interstellar wind) direction (dashed horizontal line). For the assumed interstellar wind velocity vector $|\mathbf{V}_0| = 25$ km/s pointed in the direction with ecliptic longitude $\lambda_0 = 75^\circ$, perihelion of direct atom trajectories (and zero thermal velocities in the LISM) is at point $\theta = 126^\circ$, which corresponds to ecliptic longitude $\lambda = 129^\circ$. (bottom) All-sky interstellar He atom intensity map in ecliptic coordinates for an observer moving with the Earth at point $\lambda = 129^\circ$ and helium temperature $T_0 = 8000$ K and number density $n_0 = 0.01 \text{ cm}^{-3}$ in the LISM. The instruments of the Sun-pointed spinning Earth-bound Interstellar Boundary Explorer spacecraft (top) point normally to the spin axis and thus measure atom intensities in a swath (two vertical lines) across the all-sky map. Two intensity peaks correspond to direct and indirect trajectories reaching the given point (R_0, θ). For a moving observer at $\theta = 126^\circ$ ($\lambda = 129^\circ$), helium atoms on direct trajectories are characterized by highest intensities and energies; they form the left peak at $\lambda_1 = 219^\circ$ on the sky map which is scanned across and measured by Interstellar Boundary Explorer. LISM = local interstellar medium.

Second, IBEX measurements revealed higher than expected helium atom intensities in the extended wings ($>20^\circ$ away from the peaks) of directional distributions. Such intensity enhancements could result from non-Maxwellian velocity distributions of helium at large distances from the Sun, caused by processes in the outer heliosphere (Bzowski et al., 2012, 2017; Kubiak et al., 2016; Moebius et al., 2012).

The analyses of the Ulysses and IBEX observations disregarded elastic collisions of interstellar helium atoms with solar wind ions. It had been understood since 1960s that such collisions could modify properties, effectively “heat,” interstellar atoms reaching the Earth orbit (Gruntman, 1986, 2013, and references therein). Chassefiere et al. (1986) and Gruntman (1986) identified sharp peaking of differential scattering cross sections at small scattering angles as essential for correct quantitative assessment of the effect of collisions.

Note that charge exchange collisions with the solar wind ions result in helium atom ionization which is 1.5 orders of magnitude smaller than photoionization. The corresponding charge-exchange loss rate is, similarly to photoionization, inversely proportional to the square of the heliocentric distance. Consequently, charge exchange is usually accounted for by a small adjustment of helium photoionization rate which varies by more than a factor of two during the solar cycle (Gruntman, 2013, and references therein).

Gruntman (2013) described a practical approach to account for elastic collisions based on an assumption of atoms experiencing either one or none collisions (“one-or-none collision approximation”) along trajectories to observation points at 1 AU. The calculations showed expected enhancement of intensities in the extended wings of the directional distributions, though smaller than observed by IBEX. The effect of collisions with the solar wind alpha particles turned out to be an order of magnitude smaller (Gruntman, 2013, unpublished).

Gruntman (2013) also pointed out, but not quantified, that elastic collisions with solar wind ions would broaden the core, the main “hump,” of directional intensity distributions, thus increasing derived LISM temperatures. Accounting for this heretofore disregarded effective heating of helium is particularly important because the stated uncertainties of LISM temperatures obtained from the Ulysses and IBEX observations are only a few hundred kelvins (Bzowski et al., 2015; Wood et al., 2015, 2017). In addition, the derived interstellar wind velocity vectors and temperatures are interdependent and the velocity vector provided the foundation for the conclusions of temporal and/or spatial evolution of the LISM (e.g., Frisch et al., 2013, 2015).

This work quantitatively estimates the effect of elastic collisions of interstellar helium atoms with solar wind protons and alpha particles on the inferred LISM temperatures for an experimental approach implemented in IBEX.

2. Directional Distributions of Interstellar Helium Atom Intensities

Understanding interstellar neutral atom penetration into the solar system dates back to the late 1950s and 1960s. The basic concept relies on conservation of the phase space density, as required by the Liouville’s theorem, along individual particle hyperbolic trajectories in the Sun’s gravitational field and accounting for ionization losses (e.g., Fahr, 1968, 1971; Gruntman, 1980, 2013 and foundational references therein; Meier,

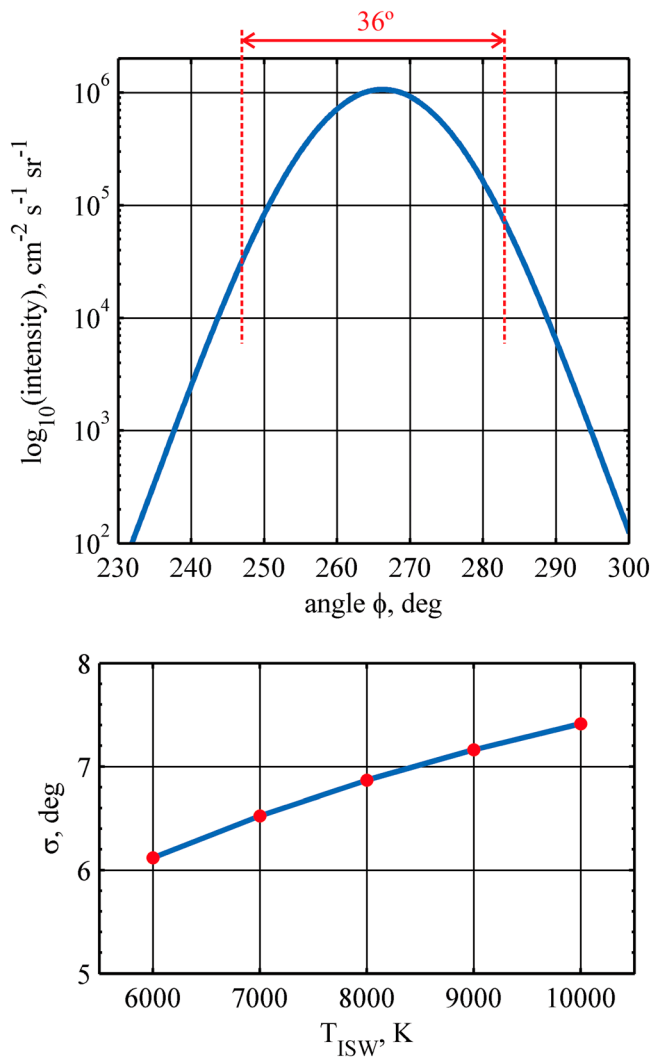


Figure 2. (top) Typical Interstellar Boundary Explorer-type swath (slice) across the peak of the directional intensity distribution for an observer at point $\theta = 126^\circ$ ($\lambda = 129^\circ$) for interstellar helium temperature $T_{\text{ISW}} = 8000$ K and velocity $|\mathbf{V}_0| = 25$ km/s. The directional angle ϕ is counted from the ecliptic south pole (Interstellar Boundary Explorer convention), with the maximum intensity at $\phi \approx 265^\circ$ for ecliptic latitude $\beta_0 = -5^\circ$ of the interstellar wind velocity vector. (bottom) Calculated dependence of standard deviation σ on the interstellar wind helium temperature T_{ISW} for the same \mathbf{V}_0 . Standard deviations of directional distributions are calculated using intensities within the 36° angular range centered on the intensity peak (top) and disregarding distribution wings outside this range. The experimentally determined σ forms the basis for obtaining helium temperature in the local interstellar medium.

1977). Various theoretical approaches emerged in 1970s for obtaining local velocity distribution functions of interstellar atoms in the solar system. Effective solar radiation forces due to scattering of solar photons do not exceed a fraction of 1% of the gravitational force acting on helium atoms and can be conveniently disregarded.

Interstellar atoms with the same velocity in the LISM reach any given point with coordinates (R, θ) in the heliosphere following two distinctly different, direct and indirect, trajectories (Figure 1). The angle θ is counted from the upwind (interstellar wind) direction. In this work, we assume the interstellar wind temperature $T_0 = 8000$ K and its velocity vector $|\mathbf{V}_0| = 25.0$ km/s pointed in the direction with ecliptic latitude $\beta_0 = -5^\circ$ and ecliptic longitude $\lambda_0 = 75^\circ$.

A point $\theta \approx 126^\circ$ ($\lambda = 129^\circ$) at the assumed circular Earth orbit with the radius $R_0 = 1$ AU is unique and of special interest for experiments. For the interstellar wind with $V_0 = 25$ km/s and $\lambda_0 = 75^\circ$, the direct atom hyperbolic trajectory is tangential to the Earth orbit at this point (trajectory perihelion), resulting in the highest velocities of interstellar helium atoms relative to the moving Earth (revolving around the Sun in the counterclockwise direction in Figure 1). These highest energies enable atom direct detection from an Earth-bound spacecraft (Gruntman, 1980, 1993; Moebius, Bochsler, et al., 2009; Moebius, Kucharek, et al., 2009; Rosenbauer et al., 1983). Therefore, the conditions for measuring intensities of interstellar helium are most favorable when the Earth is near perihelion of interstellar atom trajectories which occurs in January and February each year.

Thermal velocities of helium atoms in the unperturbed LISM far away from the Sun result in spread of directions from which the atoms reach a given observation point, forming a directional distribution of intensities in the sky. Figure 1 (bottom) shows an example (Gruntman, 2013) of a calculated all-sky intensity map for an observer moving with the Earth. Such intensity maps strongly depend on the position and velocity of an observer and on the interstellar wind velocity vector and temperature. Gruntman (2012) illustrated position-dependent evolution of all-sky maps for a moving observer and an observer at rest along the entire Earth orbit.

At the most advantageous for measurements point $\theta = 126^\circ$ ($\lambda = 129^\circ$) a moving observer would see two intensity peaks, corresponding to direct and indirect trajectories, centered at ecliptic longitudes 219° and 308° , respectively (Figure 1, bottom). The peaks are shifted by about 5° above and below the ecliptic plane because the interstellar wind velocity vector points 5° off the ecliptic plane ($\beta_0 = -5^\circ$). Atoms on direct trajectories with highest intensities and energies form the left peak on the map.

Figure 1 (top) shows the Sun-pointed spinning Earth-bound IBEX spacecraft with instruments pointed normally to the spin axis (McComas et al., 2009). As the spacecraft rotates, the instruments image a swath in the sky. For an observer at $\theta = 126^\circ$, two vertical lines on the all-sky map (Figure 1, bottom) show the observed swath of interstellar helium atom intensities. The swath crosses the intensity peak of atoms with highest energies centered at ecliptic longitude $\lambda_1 = 219^\circ$. From the observed directional distribution of intensities across the peak, IBEX derives temperature of helium atoms in the interstellar wind and thus LISM temperature T_{ISW} .

Figure 2 (top) shows an example of a calculated directional dependence of atom intensities in this IBEX-type swath (Figure 1, bottom) across the sky. The directional angle ϕ is counted from the ecliptic South Pole (IBEX

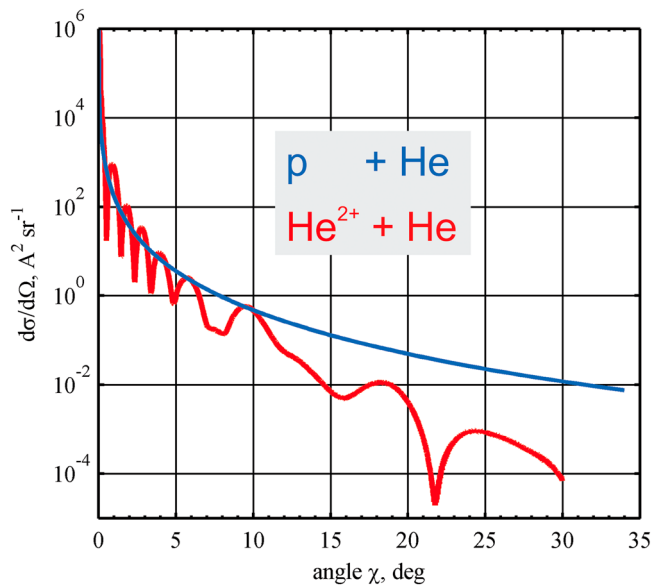


Figure 3. Differential scattering cross sections of protons (blue) and alpha particles (red) with helium atoms as a function of the scattering angle χ in the center-of-mass reference frames for the relative collision velocity 450 km/s.

convention), with the maximum intensity being at $\phi \approx 265^\circ$. The helium atom loss rate (primarily solar photoionization) is assumed to be inversely proportional to the square of the heliocentric distance. The rate at 1 AU varies from 0.6×10^{-7} to $1.7 \times 10^{-7} \text{ s}^{-1}$ during the solar cycle (Gruntman, 2013, and references therein). In this work, it is assumed to be $1.0 \times 10^{-7} \text{ s}^{-1}$.

IBEX observations show intensities in extended wings of directional intensity distributions (at angles $>20^\circ$ from the peaks) significantly larger than expected for Maxwellian distributions of atoms in the LISM (e.g., Bzowski et al., 2012). To avoid these enhanced wing intensities, the calculations of distribution standard deviations σ characterizing width of the cores of measured directional distributions are usually limited to intensities within the 36° angular range centered on the peak (Figure 2, top).

The width of the angular distribution of interstellar helium intensities in an IBEX-type sky swath depends on the LISM temperature. Figure 2 (bottom) shows the calculated dependence of the width on the interstellar wind temperature, $\sigma(T_{\text{ISW}})$. Such a dependence forms the basis for obtaining LISM temperature from IBEX measurements of helium atom intensities (e.g., Bzowski et al., 2012, 2015; Moebius, et al., 2012, 2015; Moebius, Bochsler, et al., 2009). If unaccounted for physical processes, such as elastic collisions with solar wind ions, broaden the directional

distribution and increase its standard deviation by $\Delta\sigma_0 = 0.01^\circ$, then it would correspond to the higher inferred (apparent) LISM temperature than the “real” T_{ISW} by $\Delta T_0 \approx 31 \text{ K}$.

Note that the width of directional distributions of interstellar helium intensities would slightly depend on the effective atom loss rate. For the loss rate change by a factor of 2, as possible during the solar cycle, the standard deviation σ would change by only 0.02° . This dependence on atom loss rate is commonly accounted for in interpretations of the observations. The predicted collisional heating, as discussed below, is in the $\Delta\sigma = 0.05 - 0.09^\circ$ range.

Solar radiation forces acting on interstellar helium atoms could also vary as much as a factor of 4 during the solar cycle. The effect of such variations on the width of atom intensity directional distributions in IBEX-type swaths (in a plane normal to the ecliptic) in the sky is negligible.

Elastic collisions of interstellar helium atoms with solar wind ions along their trajectories would broaden observed angular distributions of intensities. This article estimates ΔT_{ISW} increase of the derived LISM temperature due to this effect.

3. Effect of Elastic Collisions of He Atoms With Solar Wind Ions

Gruntman (2013) described in detail calculations of directional dependences, sky maps, of interstellar helium atom intensities at a given observation point when elastic collisions with solar wind ions take place. Briefly, one selects a velocity vector of a helium atom at an observation point and analytically reconstructs the atom trajectory to large heliocentric distances (say, 100 AU) in the unperturbed LISM. In the absence of atom losses and collisions, the phase space density of interstellar helium is conserved along particle trajectories, as required by the Liouville’s theorem. The losses can be accounted for in a particularly simple manner for an ionization rate inversely proportional to the square of the heliocentric distance.

Then, one calculates a probability for a collision to occur along the atom trajectory at a certain distance from the observation point. Scattering in the collision gives a distribution of probabilities of directions and velocities of atoms arriving to the collision point from the LISM. Tracing trajectories of these atoms further back into the LISM with the corresponding local phase space densities and accounting for losses allow one to obtain intensity of atoms with the initially selected velocity vector at the given observation point. Finally, varying velocity vectors of atoms at the observation point, the distributions of helium atom intensities and velocities at this point are calculated.

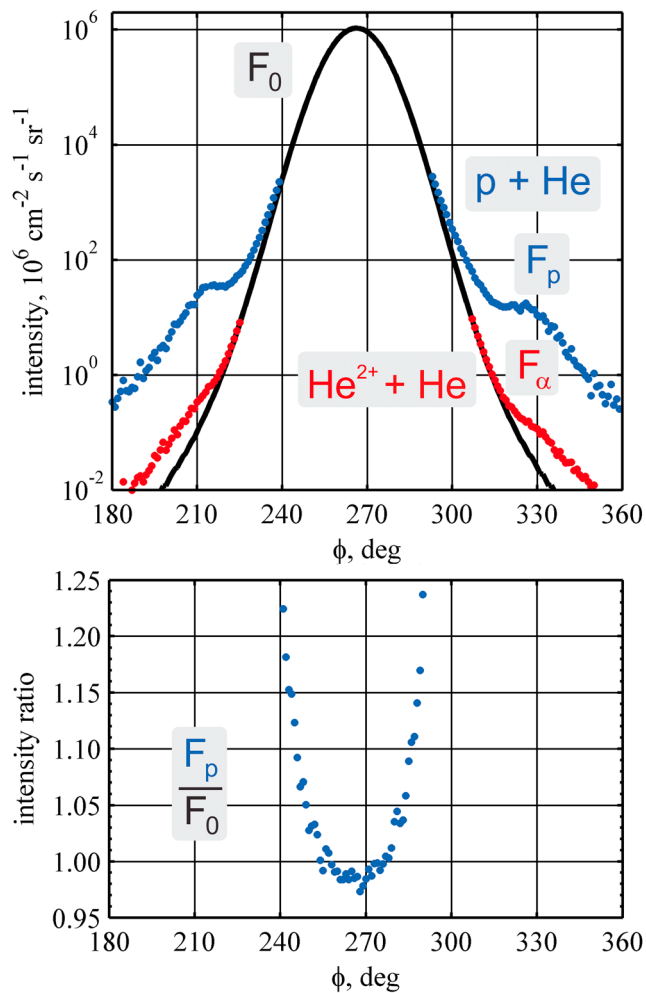


Figure 4. (top) Directional dependences of interstellar helium atom intensities at $\theta = 126^\circ$ ($\lambda = 129^\circ$) for a moving with the earth observer for helium atoms without any collisions (F_0 , black), with collisions with the solar wind protons only (F_p , blue), and with collisions with the solar wind alpha particles only (F_α , red). (bottom) The ratio F_p/F_0 of intensities with collisions with the solar wind protons and without collisions.

tons are two orders of magnitude higher than those due to collisions with alpha particles. IBEX-observed intensities in the extended wings (Bzowski et al., 2012) are about one order of magnitude higher than intensities due to elastic collisions shown in Figure 4 (Gruntman, 2013). Consequently, it seems that elastic collisions cannot explain the observations which opens a way, as argued by, for example, Bzowski et al. (2017), to interpreting enhanced intensities in the wings as a signature of non-Maxwellian interstellar helium atom distributions at large heliocentric distances, perhaps caused by charge exchange collisions in the outer heliosphere.

Broadening of the core of the angular distributions due to collisions can be seen in Figure 4 (bottom), which shows the ratio F_p/F_0 of intensities with and without collisions as a function of the directional angle ϕ . The peak intensity of the distribution with collisions is about 2% smaller and intensities are 10% higher 20° away from the peak. The effect of collisions with the solar wind alpha particles in the distribution core is one-two orders of magnitude smaller than that of collisions with the protons.

The width of the angular distributions is larger when collisions with the protons are present compared to the width without collisions. The corresponding increase in standard deviation of the angular distributions is $\Delta\sigma \approx 0.058^\circ$. The deviations are calculated using only intensities within the 36° angular range centered on the peak intensity (as commonly done for IBEX data). This broadening corresponds to increase of the

Gruntman (2013) discussed in detail physical approximations used in calculations. In particular, scattering on angles smaller than a certain minimal angle, χ_{MIN} , are disregarded. Here we consider scattering on angles larger than 0.3° and 0.4° (in the center-of-mass reference frame of colliding particles) in collisions of solar wind protons and alpha particles, respectively, with interstellar helium atoms. The average number of such collisions experienced by helium atoms on their trajectories to the observation point at 1 AU under typical solar wind conditions is $\gamma_0 = 0.15 - 0.3$. Such a small number of average collisions justify the one-or-none collision approximation (Gruntman, 2013). This simplification allows calculation of sky maps considering interstellar helium atoms moving either without collisions or experiencing only one collision along their trajectories. The disregarded collisions on smaller than minimal angles would average 0.7–1.4 along atom trajectories. The contribution of such collisions to heating of interstellar helium does not exceed 10–20 K, as discussed below.

Liu et al. (2012) and Gruntman (2013) described the essential quantum-mechanical formalisms and calculations of helium atom elastic differential scattering in collisions with alpha particles and protons, respectively. Figure 3 shows the calculated differential scattering cross sections for alpha particles (C. H. Liu, private communications, 2012, 2013) and protons (Gruntman, 2013) for a 450-km/s collision velocity.

Elastic collisions of interstellar helium with solar wind ions result in increased intensity in the wings of the directional distributions and in broadening (heating) of the distribution core (Gruntman, 1986, 2013). Figure 4 (top) shows the calculated angular distributions of intensities $F_0(\phi)$ in an IBEX-type swath in the sky for helium atoms without collisions (black curve); $F_p(\phi)$ with collisions with the solar wind protons only (blue); and $F_\alpha(\phi)$ with collisions with solar wind alpha particles only (red) at point $\theta = 126^\circ$ ($\lambda = 129^\circ$). We assume the radially expanding solar wind with the constant velocity $V_{\text{SW}} = 450 \text{ km/s}$, number density of protons $n_p = 5 \text{ cm}^{-3}$, and the corresponding flux density $f_{\text{SW}} = n_p V_{\text{SW}} = 2.25 \times 10^8 \text{ cm}^{-2} \text{ s}^{-1}$ at 1 AU; the alpha particle number density is 5% of that of the protons.

Solar wind protons dominate collisional effects. In the far wings $>30^\circ$ away from the distribution peak, intensities due to collisions with pro-

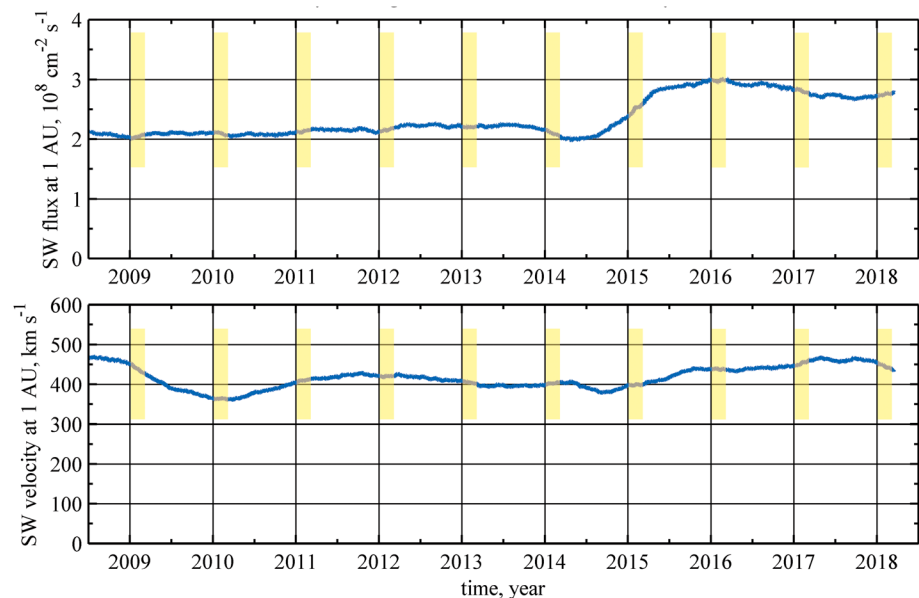


Figure 5. Trailing 365-day sliding averages of the solar wind flux densities (top) and velocities (bottom) at 1 AU. Trailing average means that the shown parameter at a certain day is averaged during the preceding 365-day interval. Vertical semitransparent rectangles show periods in January and February of each year that are most favorable for observation of interstellar neutral helium atom intensities by Interstellar Boundary Explorer. Original daily data from OMNI (<https://omniweb.gsfc.nasa.gov>; retrieved on 15 April 2018). SW = solar wind.

inferred temperature of interstellar helium in the LISM by $\Delta T_p \approx 180$ K. The corresponding LISM temperature increase due to collisions with the solar wind alpha particles is $\Delta T_\alpha \approx 7$ K. Estimates also show that disregarded collisions on angles smaller than the minimal angles χ_{MIN} would result in increases of inferred LISM temperatures not exceeding 10 K. Consequently, the total increase of the inferred LISM temperature due to heretofore unaccounted for heating of interstellar helium atoms in elastic collisions with the solar wind protons and alpha particles would be close to $\Delta T_{\text{ISW}} \approx 200$ K.

4. Discussion and Conclusions

Elastic collisions of interstellar helium atoms with solar wind ions cause broadening of directional distributions of interstellar helium atom intensities in the IBEX-type observations. Collisions with the solar wind protons are primarily responsible for this effect.

Broadening of directional distributions leads, if not corrected, to higher values of inferred LISM temperatures by approximately $\Delta T_{\text{ISW}} \approx 200^\circ$. In other words, interstellar helium and LISM are about 200 K cooler than they appear based on the temperature derived from direct detection of interstellar helium atoms intensities because of collisions. Note that this effect would depend on the solar wind conditions.

Most atom collisions occur on the portion of their trajectories close to the Sun. Gruntman (2013) showed that for a given trajectory the average number of collisions is proportional to the angle between the incoming radial asymptote and the radius-vector to a point of interest. For a hyperbolic trajectory reaching its perihelion at $\theta = 126^\circ$ and 1 AU, approximately 90% of the collisions take place within 7–8 AU from the Sun. The interstellar He atom velocity varies from 29 km/s at 8 AU to 49 km/s at 1 AU. The atom thus crosses this distance in about 1 year. The varying solar wind conditions, averaged over that year, would result in different collision rates of helium atoms and determine the magnitude of the predicted effect.

Figure 5 shows daily variations of the trailing 365-day sliding averages of the solar wind flux densities and velocities at 1 AU during the IBEX mission from its launch in December 2008. The averages are derived from the OMNI (<https://omniweb.gsfc.nasa.gov>) daily database for the ecliptic solar wind. (Note that trajectories of

helium atoms reaching 1 AU are within $\pm 30^\circ$ in ecliptic latitude.) Trailing average means that the shown parameter at a certain day is averaged during the preceding 365-day interval.

The semitransparent vertical rectangles (Figure 5) show periods of January and February of each year that are most favorable for observation of interstellar helium atom intensities by IBEX. One can see that the solar wind flux densities vary by almost a factor of 1.5, from $(2.0 - 3.0) \times 10^8 \text{ cm}^{-2} \text{ s}^{-1}$, in these time intervals during the IBEX mission. The obtained above increase of apparent temperature $\Delta T_{\text{ISW}} \approx 200^\circ$ corresponds to the assumed solar wind flux density $2.25 \times 10^8 \text{ cm}^{-2} \text{ s}^{-1}$ at 1 AU.

The average number of collisions experienced by interstellar helium atoms is approximately proportional to the flux density of the solar wind protons at 1 AU (Gruntman, 2013). It would vary from 0.15 to 0.3 for the selected minimal scattering angles χ_{MIN} , justifying use of the one-or-none collision approximation. If one disregards dependence of differential scattering on the solar wind velocity then ΔT_{ISW} would simply scale with the solar wind flux density. So depending on the solar wind conditions during 1 year preceding the measurements, the increase of inferred LISM temperatures would be in the $\Delta T_{\text{ISW}} = 175 - 270 \text{ K}$ range. The corresponding increase in standard deviations of directional distributions is $\Delta\sigma = 0.05 - 0.09^\circ$.

Note that the observation conditions in the early 2011, 2014, and 2016 are characterized by similar solar wind velocities (and thus similar differential cross sections) but significantly different, by a factor of 1.5, solar wind flux densities. Therefore, these three years of observations offer an opportunity for search of differences in inferred LISM temperatures which may directly reveal the effect of collisional heating of interstellar helium in the solar system. Another promising set of observational seasons is years 2009 and 2016, 2017, and 2018.

To conclude, the predicted effect of collisional heating of interstellar helium is comparable to current uncertainties of determining LISM temperatures from the Ulysses and IBEX measurements (Bzowski et al., 2015; Wood et al., 2015). Therefore, it may be possible to discover the effect in the IBEX data, particularly by comparison of observations during the 2011, 2014, and 2016 seasons and during 2009, 2016, 2017, and 2018. Accounting for collisional heating may also become important for reconciling values of the LISM temperatures obtained from Ulysses and IBEX observations (Wood et al., 2015).

Acknowledgments

This work is supported, in part, by NASA's IBEX program. I would like to thank Ratko Janev and Chun-Hua Liu for discussions of collisional processes and calculating differential scattering cross sections for alpha particle collisions with atomic helium. The OMNI data were obtained from the GSFC/SPDF OMNIWeb interface at <https://omniweb.gsfc.nasa.gov>.

References

- Bzowski, M., Kubiak, M. A., Czechowski, A., & Grygorczuk, J. (2017). The helium warm breeze in IBEX observations as a result of charge exchange collisions in the outer heliosheath. *The Astrophysical Journal*, 845(1), 15. <https://doi.org/10.3847/1538-4357/aa7ed5>
- Bzowski, M., Kubiak, M. A., Moebius, E., Bochsler, P., Leonard, T., Heitzler, D., et al. (2012). Neutral interstellar helium parameters based on IBEX-Lo observations and test particle calculations. *The Astrophysical Journal Supplement Series*, 198(2). <https://doi.org/10.1088/0067-0049/198/2/12>
- Bzowski, M., Swaczyna, P., Kubiak, M. A., Sokol, J. M., Fuselier, S. A., Galli, A., et al. (2015). Interstellar neutral helium in the heliosphere from IBEX observations. III. Mach number of the flow, velocity vector, and temperature from the first six years of measurements. *The Astrophysical Journal Supplement Series*, 220(2), 28. <https://doi.org/10.1088/0067-0049/220/2/28>
- Chassefiere, E., Bertaux, J. L., & Sidis, V. (1986). Elastic collisions of solar wind protons with interstellar neutrals (H and He) inside the heliosphere: A new approach. *Astronomy and Astrophysics*, 169, 298–304.
- Fahr, H. J. (1968). On the influence of neutral interstellar matter on the upper atmosphere. *Astrophysics and Space Science*, 2(4), 474–495. <https://doi.org/10.1007/BF02175923>
- Fahr, H. J. (1971). The interplanetary hydrogen cone and its solar cycle variations. *Astronomy and Astrophysics*, 14, 263–275.
- Frisch, P. C., Bzowski, M., Drews, C., Leonard, T., Livadiotis, G., McComas, D. J., et al. (2015). Correcting the record on the analysis of IBEX and STEREO data regarding variations in the neutral interstellar wind. *The Astrophysical Journal*, 801(1), 61. <https://doi.org/10.1088/0004-637X/801/1/61>
- Frisch, P. C., Bzowski, M., Livadiotis, G., McComas, D. J., Moebius, E., Mueller, H. R., et al. (2013). Decades-long changes of the interstellar wind through our solar system. *Science*, 341(6150), 1080–1082. <https://doi.org/10.1126/science.1239925>
- Fuselier, S. A., Bochsler, P., Chornay, D., Clark, G., Crew, G. B., Dunn, G., et al. (2009). The IBEX-Lo sensor. *Space Science Reviews*, 146(1–4), 117–147. <https://doi.org/10.1007/s11214-009-9495-8>
- Gruntman, M. (1980). Interstellar helium at Earth orbit (Preprint 543). Moscow USSR: Space Research Institute (IKI), USSR Academy of Sciences.
- Gruntman, M. (1986). Concerning the problem of collisional heating of the interstellar helium by solar wind protons. *Planetary and Space Science*, 34(4), 387–389. [https://doi.org/10.1016/0032-0633\(86\)90145-5](https://doi.org/10.1016/0032-0633(86)90145-5)
- Gruntman, M. (1989). MASTIF: Mass analysis of secondaries by time-of-flight technique. New approach to secondary ion mass spectrometry. *The Review of Scientific Instruments*, 60(10), 3188–3194. <https://doi.org/10.1063/1.1140550>
- Gruntman, M. (1993). A new technique for in situ measurement of the composition of interstellar gas in the heliosphere. *Planetary and Space Science*, 41(4), 307–319. [https://doi.org/10.1016/0032-0633\(93\)90026-X](https://doi.org/10.1016/0032-0633(93)90026-X)
- Gruntman, M. (1997). Energetic neutral atom imaging of space plasmas. *The Review of Scientific Instruments*, 68(10), 3617–3656. <https://doi.org/10.1063/1.1148389>
- Gruntman, M. (2012, October 27). Interstellar helium flux at 1 AU, YouTube video (8 min.). Retrieved from <https://youtu.be/oQnjwHPxJfg> on February 12, 2018

- Gruntman, M. (2013). Elastic collisions of interstellar helium atoms with solar wind protons. *Journal of Geophysical Research: Space Physics*, 118, 1366–1378. <https://doi.org/10.1002/jgra.50199>
- Katushkina, O. A., Izmodenov, V. V., Wood, B. E., & McMullin, D. R. (2014). Neutral interstellar helium parameters based on ULYSSES/GAS and IBEX-LO observations: What are the reasons for the differences? *The Astrophysical Journal*, 789(1), 80. <https://doi.org/10.1088/0004-637X/789/1/80>
- Kubiak, M. A., Swaczyna, P., Bzowski, M., Sokol, J. M., Fuselier, S. A., Galli, A., et al. (2016). Interstellar neutral helium in the heliosphere from IBEX observations. IV. Flow vector, Mach number, and abundance of the Warm Breeze. *The Astrophysical Journal Supplement Series*, 223, 35. <https://doi.org/10.3847/0067-0049/223/2/35>
- Lallement, R., & Bertaux, J. L. (2014). On the decades-long stability of the interstellar wind through the solar system. *Astronomy and Astrophysics*, 565, A41. <https://doi.org/10.1051/0004-6361/201323216>
- Lee, M. A., Kucharek, H., Mobius, E., Wu, X., Bzowski, M., & McComas, D. (2012). An analytical model of interstellar gas in the heliosphere tailored to Interstellar Boundary Explorer observations. *The Astrophysical Journal Supplement*, 198(2), 10. <https://doi.org/10.1088/0067-0049/198/2/10>
- Lee, M. A., Moebius, E., & Leonard, T. W. (2015). The analytical structure of the primary interstellar helium distribution function in the heliosphere. *The Astrophysical Journal Supplement*, 220(2), 23. <https://doi.org/10.1088/0067-0049/220/2/23>
- Liu, C. H., Wang, J. G., & Janev, R. K. (2012). Single- and double-charge transfer in slow He^{2+} -He collisions. *Journal of Physics B: Atomic, Molecular and Optical Physics*, 45(23), 235203. <https://doi.org/10.1088/0953-4075/45/23/235203>
- McComas, D. J., Allegrini, F., Bochsler, P., Bzowski, M., Collier, M., Fahr, H., et al. (2009). IBEX—Interstellar Boundary Explorer. *Space Science Reviews*, 146(1–4), 11–33. <https://doi.org/10.1007/s11214-009-9499-4>
- McComas, D. J., Bzowski, M., Fuselier, S. A., Frisch, P. C., Galli, A., Izmodenov, V. V., et al. (2015). Local interstellar medium: Six years of sampling by IBEX. *The Astrophysical Journal Supplement*, 220(2), 22. <https://doi.org/10.1088/0067-0049/220/2/22>
- Meier, R. R. (1977). Some optical and kinetic properties of the nearby interstellar gas. *Astronomy and Astrophysics*, 55, 211–219.
- Moebius, E., Bochsler, P., Bzowski, M., Crew, G. B., Funsten, H. O., Fuselier, S. A., et al. (2009). Direct observations of interstellar H, He, and O by the Interstellar Boundary Explorer. *Science*, 326(5955), 969–971. <https://doi.org/10.1126/science.1180971>
- Moebius, E., Bochsler, P., Bzowski, M., Heirtzler, D., Kubiak, M. A., Kucharek, H., et al. (2012). Interstellar gas flow parameters derived from Interstellar Boundary Explorer-Lo observations in 2009 and 2010: Analytical analysis. *The Astrophysical Journal Supplement*, 198(2). <https://doi.org/10.1088/0067-0049/198/2/11>
- Moebius, E., Bzowski, M., Frisch, P. C., Fuselier, S. A., Heirtzler, D., Kubiak, M. A., et al. (2015). Interstellar flow and temperature determination with IBEX: Robustness and sensitivity to systematic effects. *The Astrophysical Journal Supplement*, 220(2), 24. <https://doi.org/10.1088/0067-0049/220/2/24>
- Moebius, E., Kucharek, H., Clark, G., O'Neill, M., Petersen, L., Bzowski, M., et al. (2009). Diagnosing the neutral interstellar gas flow at 1 AU with IBEX-Lo. *Space Science Reviews*, 146(1–4), 149–172. <https://doi.org/10.1007/s11214-009-9498-5>
- Rosenbauer, H., Fahr, H. J., Keppler, E., Witte, M., Hemmerich, P., Lauche, H., et al. (1983). The ISPM interstellar neutral-gas experiment. *ESA Special Publication*, ESA, SP-1050, 123–139.
- Witte, M. (2004). Kinetic parameters of interstellar neutral helium. Review of results obtained during one solar cycle with the Ulysses/GAS-instrument. *Astronomy and Astrophysics*, 426(3), 835–844. <https://doi.org/10.1051/0004-6361:20035956>
- Witte, M., Banaszkiewicz, M., & Rosenbauer, H. (1996). Recent results on the parameters of the interstellar helium from the Ulysses/GAS experiment. *Space Science Reviews*, 78(1–2), 289–296. <https://doi.org/10.1007/BF00170815>
- Witte, M., Bleszynski, S., Banaszkiewicz, M., & Rosenbauer, H. (1999). Sputtering efficiency of LiF surfaces on impact of low energy neutral helium 20–80 eV: Calibration of the interstellar neutral helium instrument on ULYSSES. *The Review of Scientific Instruments*, 70(11), 4404–4411. <https://doi.org/10.1063/1.1150085>
- Witte, M., Rosenbauer, H., Keppler, E., Fahr, H., Hemmerich, P., Lauche, H., et al. (1992). The interstellar neutral-gas experiment on ULYSSES. *Astronomy & Astrophysics, Supplement Series*, 92, 333–348.
- Wood, B. E., Mueller, H. R., & Witte, M. (2015). Revisiting Ulysses observations of interstellar helium. *The Astrophysical Journal*, 801(1), 62. <https://doi.org/10.1088/0004-637X/801/1/62>
- Wood, B. E., Mueller, H. R., & Witte, M. (2017). A Ulysses detection of secondary helium neutrals. *The Astrophysical Journal*, 851(1), 35. <https://doi.org/10.3847/1538-4357/aa9889>